

ELECTRICAL CONDUCTIVITY OF SINTERED LSM CERAMICS

ELEKTRIČNA PREVODNOST SINTRANE LSM-KERAMIKE

Marjan Marinšek

University of Ljubljana, Faculty of Chemistry and Chemical Technology, Aškerčeva 5, Ljubljana, Slovenia
marjan.marinsen@fkkt.uni-lj.si

Prejem rokopisa – received: 2008-10-13; sprejem za objavo – accepted for publication: 2008-11-26

The carbonate co-precipitation route was applied for batch $\text{La}_{0.85}\text{Sr}_{0.15}\text{MnO}_3$ (LSM) preparation as an alternative synthesis method to the solid-state reaction. Because co-precipitation is a wet-chemistry solution process, the maximum LSM homogeneity was achieved. The microstructural characteristics, such as the porosity and grain size of the prepared LSM elements, were controlled by subjecting the green bodies to various sintering conditions. The LSM sintered bodies with relative sintered densities as high as 95 % were prepared at sintering temperatures not higher than 1100 °C. The microstructure of the prepared LSM was characterized by digital online image analysis and the microstructural parameters were determined for the ceramic phase as well as for the porosity. The electrical characteristics of the sintered LSM elements were, for the first time in the literature, described with respect to a model for the sine-wave approximation of the conductivity change for porous materials. The observed results of the relative conductivity σ/σ_0 vs. the relative density ρ/ρ_0 dependence were essentially consistent with the sine-wave approximation. As an absolute value, the highest $\sigma = 65 \text{ S/cm}$ at 800 °C was measured for a sample with $\rho/\rho_0 = 99.58 \%$.

Key words: LSM co-precipitation, microstructure, electrical conductivity, sine-wave approximation of conductivity

$\text{La}_{0.85}\text{Sr}_{0.15}\text{MnO}_3$ (LSM) je bil pripravljen po metodi karbonatne koprecipitacije kot alternativa metodi reakcije v trdnem. Z uporabo koprecipitacijske metode kot ene izmed tehnik mokre kemije nam je uspelo pripraviti zelo homogene LSM-prahove. Mikrostrukturne lastnosti končnih, pripravljenih LSM-elementov, kot sta poroznost in velikost zrn, smo spreminjali s sintranjem LSM-surovcev pri različnih pogojih. Uspelo nam je pripraviti sintrane LSM-elemente z relativno sintrano gostoto $\approx 95 \%$ pri temperaturah sintranja, ki niso bile višje kot 1100 °C. Bolj podrobna karakterizacija mikrostrukture sintranih elementov je bila opravljena z analizo digitalnih slik. Električne lastnosti sintranih LSM-elementov smo pojasnili s teoretičnim modelom vrtenine za opis električne prevodnosti porozne keramike, kar je tudi prvi tovrsten opis LSM-keramike. Rezultati določitve relativne prevodnosti σ/σ_0 LSM-keramike kot funkcije njene relativne gostote ρ/ρ_0 relativno dobro sledijo predlaganemu teoretičnemu modelu. Najvišjo absolutno izmerjeno vrednost električne prevodnosti $\sigma = 65 \text{ S/cm}$ pri 800 °C je imel vzorec z relativno gostoto $\rho/\rho_0 = 99,58 \%$.

Ključne besede: LSM-koprecipitacija, mikrostruktura, električna prevodnost, "sine-vawe" model prevodnosti

1 INTRODUCTION

Lanthanum strontium manganite ($\text{La}_{1-x}\text{Sr}_x\text{MnO}_3$, LSM) has been extensively used as a cathode material for solid-oxide fuel cells (SOFCs). It offers a high electronic conductivity, a high catalytic activity for oxygen reduction as well as chemical and thermal compatibility with the yttria-stabilized zirconia (YSZ) electrolyte at the operating temperature^{1,2}. In the present generation of SOFCs, the nominal composition of $\text{La}_{1-x}\text{Sr}_x\text{MnO}_3$ ($x < 0.2$) is normally used^{3,4}. The use of LSM-based cathode materials depends not only on their chemical, structural and thermodynamic characteristics, but also on their final microstructure, grain size, pore size and pore-size distribution⁵⁻⁷.

Various preparation techniques have been reported for LSM synthesis. In general, perovskite manganites are synthesized at high temperatures using a standard ceramic technique. However, when utilizing a solid-state reaction for LSM preparation, the homogeneity and final microstructure of the material are more difficult to control, due to the fact that the conventional ceramic synthesis process is based on the diffusion of components in the solid state at high temperatures. In this respect,

several preparation techniques based on solution chemistry methods, such as the citrate-gel process⁸⁻¹², the sol-gel process¹³⁻¹⁵, combustion syntheses^{16,17} and the co-precipitation technique^{18,19} have also been tested for the preparation of highly homogenous and fine LSM powders.

The characterization of LSM and some other perovskite powders such as SOFC cathodes or oxygen membranes prepared by different chemical routes was made by Sfeir et al.²⁰, while a comprehensive study of the effect of the synthesis route on the catalytic activity of LSM was performed by Bell et al.²¹. The results of these studies implied that the carbonate co-precipitation synthesis route is especially interesting since it delivers a finer powder with a more homogeneous composition and surface structure and is, thus, more suited to mixed-conductor applications in SOFC systems. The groundwork of the co-precipitation method for the LSM preparation was done by Tanaka et al., where Na_2CO_3 was used as the precipitating agent²². However, one of the serious drawbacks of the method is the incorporation of Na^+ ions into the precipitate due to the use of Na_2CO_3 . Another co-precipitation-based LSM preparation was developed

by Ghosh et al.,¹⁹ using ammonium carbonate as the precipitating agent.

LSM is a perovskite oxide ABO_3 where the La^{3+} ions at the A-sites are partially substituted by Sr^{2+} ions. $LaMnO_3$ is a p-type semiconductor due to the small polaron hopping of holes²³ between the Mn^{3+} and Mn^{4+} ions. The doping of Sr into $LaMnO_3$ increases the electrical conductivity considerably because of the increased number of holes²⁴. However, in order to serve as a cathode material in an operating fuel cell, besides the appropriate electro-catalytic properties, the LSM also has to exhibit suitable microstructure characteristics, including $\approx 30\%$ open porosity. Changing the porosity, going from a dense to a more porous structure, will again alter some of the electrical characteristics of the material, since the apparent conductivity of sintered materials is sensitive to their relative density. To describe the relationship between the conductivity of the porous material and its relative density, a novel mathematical approach was proposed²⁵. In this new method of interpretation, where as a first approximation, porous material is represented by a uniaxial string of spheres along the direction of the potential gradient and then remodeled into a rotating body, the conductivity of highly porous ceramic materials can be expressed with a model of a rotating sine-wave function. By changing the ratio of the contribution of two sine-waves, one representing the shape of each grain and the other the shape of the bottleneck between the particles, the change of the electrical conductivity σ vs. the change of the material's relative density ρ/ρ_0 can be represented.

In the present work, the carbonate co-precipitation route for batch LSM preparation was applied. Being a solution process, the maximum product homogeneity with minimum secondary-phase addition can be achieved. The aim of the study is a description of the electrical conductivity behavior of the prepared LSM bodies with respect to the material's microstructure characteristics. For the first time, the specific electrical conductivity of porous LSM is explained with the model of a rotating sine-wave function.

2 EXPERIMENTAL PROCEDURE

In order to prepare stock solutions of 0.5-M lanthanum nitrate and strontium nitrate, lanthanum oxide (La_2O_3) and strontium carbonate ($SrCO_3$) were separately, carefully dissolved in concentrated nitric acid, while manganous nitrate ($Mn(NO_3)_2 \cdot 4H_2O$) was dissolved in distilled water. For the $La_{0.85}Sr_{0.15}MnO_3$ preparation, predetermined amounts of each solution were then mixed. The mixed solution was added drop-wise to a precipitating bath containing an aqueous solution of ammonium carbonate in which the amount of ammonium carbonate was in 50 % excess for the complete precipitation of the mixed La-Mn-Sr-precursor. The pH of the precipitating bath was kept constant at 8.0 by

small additions of aqueous ammonia. The temperature of the reaction mixture in the precipitating bath was adjusted to 65 °C and kept constant. The precipitation reaction took place under a CO_2 atmosphere to prevent any undesired oxidation of the manganese to MnO_2 . The reaction time for the complete co-precipitation process was approximately 3 h.

Typical quantities of the initial precursors consumed in one cycle of the bath precipitation were 100 g of $(NH_4)_2CO_3$ dissolved in 2.5 L of H_2O , 854 mL of 0.5-M Mn-precursor solution, 363 mL of 0.5-M La-precursor solution, and 128 mL of 0.5-M Sr-precursor solution. Such a reaction mixture yielded approximately 100 g of the final, calcined LSM powder.

The filtered precipitate was washed several times with a 0.125-M aqueous ammonium-carbonate solution and then dried first at room temperature in a CO_2 atmosphere for several hours and afterwards for six hours at 110 °C in air. Prior to calcination in a muffle furnace at 1000 °C for one hour, the dried powder was ground in an agate mortar. Calcined LSM powders were then wet milled in a ball mill in isopropanol. To achieve a higher morphological homogeneity the wet-milled powders were further subjected to attritor milling.

Thus prepared, the LSM powders were pressed into tablets ($\Phi = 6$ mm, $h \sim 4$ mm, $P = 200$ MPa) and sintered at various temperatures from 1000 °C to 1330 °C for one hour.

The samples were characterized with the X-ray powder-diffraction technique using a D4 ENDEAVOR diffractometer. The shrinkage during the sintering was measured with a LEITZ WETZLAR heating microscope. After sintering and polishing the samples were thermally etched and analyzed by SEM (Zeiss FE SUPRA 35 VP). The quantitative analysis of the microstructures was performed using a Zeiss KS300 3.0 image analyzer. In order to get accurate data on the electrical resistivity of the prepared and sintered pellets as a function of temperature, the four-point electrical resistivity method was used.

3 RESULTS AND DISCUSSION

The precipitated and calcined powders were submitted for an XRD examination (**Figure 1**). For XRD study purposes the calcination of the precursor carbonate-hydroxide powder was carried out in the temperature range 1000–1400 °C. According to **Figure 1**, calcination at 1000 °C is quite sufficient for a complete perovskite LSM phase formation. Another apparent characteristic from the XRD results is that only traces of the residual secondary phases La_2O_3 or $La(OH)_3$ are still present after the calcination ($La(OH)_3$ resulting from the reaction of the La_2O_3 with moisture). Additionally, no Mn-oxide secondary phases were detected with the XRD analysis. During the calcination at higher temperatures (1100–1400 °C) the secondary phases are completely

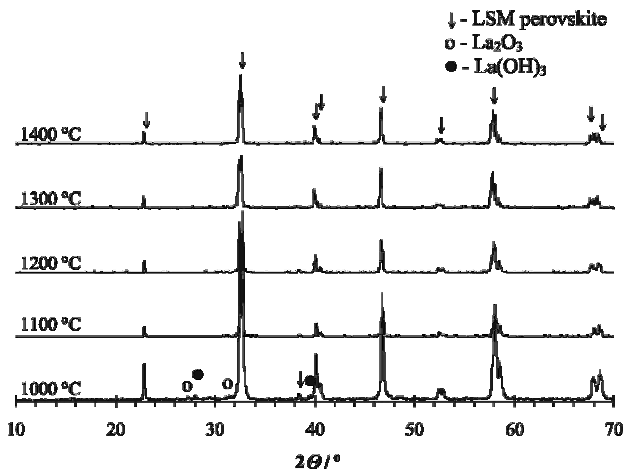


Figure 1: XRD patterns of the synthesized powders calcined at different temperatures

Slika 1: Praškovni posnetki sintetiziranih vzorcev, kalciniranih pri različnih temperaturah

dissolved in the perovskite structure. The relatively small amount of secondary phases in the sample calcined up to 1000 °C makes the co-precipitation method favorable when compared to synthesis processes that are based on the diffusion of components in the solid state. Namely, if the solid-state reaction is employed for the LSM preparation, the amount of secondary phases is normally greater.

At this point, it is necessary to mention that secondary phases may nevertheless appear in the LSM structure, even in the case when the calcination temperature exceeds 1100 °C. Specifically, a precise SEM analysis revealed that calcination or sintering of the prepared LSM at temperatures above 1100 °C caused the reprecipitation of MnO_2 at the LSM grain-boundary region (**Figure 2**). The amount of reprecipitated MnO_2 at 1100 °C is relatively low (the volume fraction below 1 % of the material) but is increased to 3.9 % when the material is thermally treated at 1330 °C for 1 h.

One of the principal characteristics LSM has to exhibit is sintering at relatively low temperatures (less than 1200 °C). This is very important from the applica-

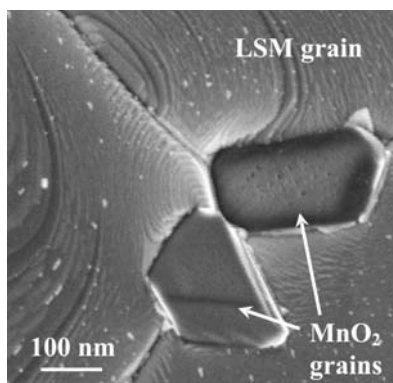


Figure 2: Microstructure of LSM sample thermally treated at 1330 °C for 1 hour

Slika 2: Mikrostruktura LSM-vzorca, obdelanega pri 1330 °C 1 h

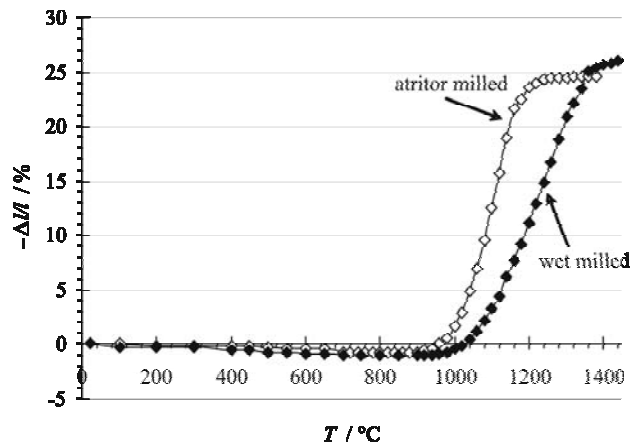


Figure 3: Shrinkage curves of LSM tablets after powder wet milling or after additional attritor milling

Slika 3: Krivulje sintranja LSM-surovca po mokrem mletju prahu oziroma po dodatnem atritorskem mletju prahu

tion point of view. If the material is used as a cathode in SOFC systems and co-sintered with other cell layers, then sintering at temperatures above 1200 °C may cause some highly undesirable reactions with neighboring materials^{26,27}. For this reason, the morphological homogeneity of LSM powders is essential for achieving material densification at relatively low temperatures. During LSM sinterability tests, the best results were achieved when a combination of milling methods was used (grinding in an agate mortar, wet milling in a ball mill and attritor milling). After wet milling in a ball mill in isopropanol, the average particle size d_{av} was determined to be 2.45 μm (standard deviation σ 1.98 μm). After 3 hours of additional attritor milling d_{av} was lowered to 0.57 μm (σ 0.52 μm). Such a combination of homogenization operations substantially lowered the sintering temperature of the LSM tablets (**Figure 3**).

After successfully reducing the sintering temperature, a series of tablets in the green state was prepared and sintered at various temperatures in order to alter the densities of the sintered elements. Prior to establishing the LSM's electrical characteristics with respect to its microstructure, a complete, quantitative microstructure analysis was performed on sintered and polished elements (**Table 1**, **Figure 4**). According to the results summarized in Table 1, rather dense elements with relative densities of more than 92 % can be prepared at sintering temperatures T_s as low as 1090 °C. This is of prime importance when multilayered structures of SOFCs are prepared; it is very important that the material is capable of densification at relatively low temperatures, resulting in good particle-to-particle connections, especially in cases where a high electrical conductivity is required.

In contrast to the sintered density, the porosity of the sintered elements decreased with an increased sintering temperature. The elements' porosity was determined from the material density as the geometrical porosity ε (ε

Table 1: Microstructural parameters of the sintered LSM bodies**Tabela 1:** Mikrostrukturne značilnosti sintranih LSM-tabletk

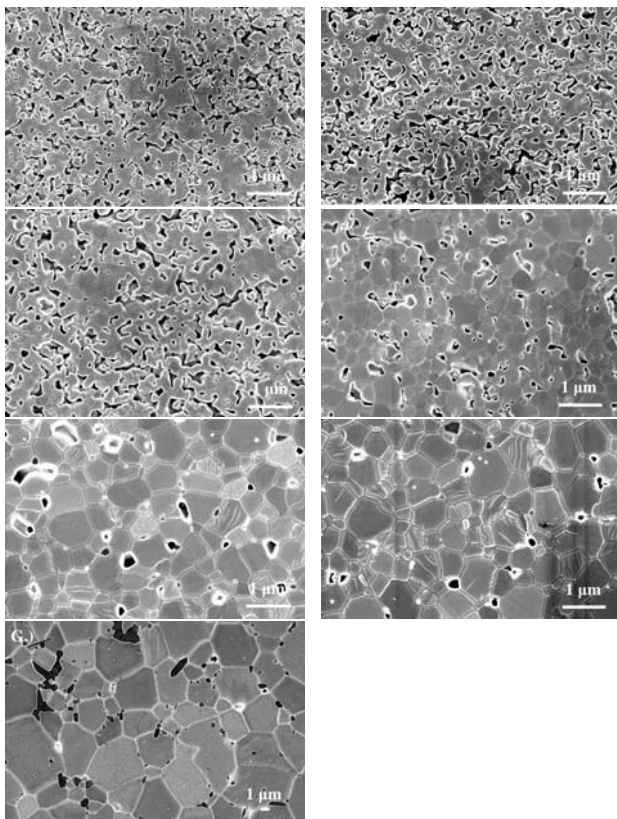
sample	A	B	C	D	E	F	G
sintering temperature $T_s / ^\circ\text{C}$	1000	1015	1024	1060	1090	1100	1330
relative sintered density $\rho_s / \%$	57.3	65.8	70.1	83.0	92.7	94.1	98.2
porosity (geometrical) $\varepsilon / \%$	42.7	34.2	29.9	17.0	7.3	5.9	1.8
porosity (microstructural) $\varepsilon' / \%$	43.2	28.6	25.4	15.9	6.0	4.4	0.9
mean particle diameter $\bar{d} \cdot 10^2 / \mu\text{m}$	5.7	8.9	20.0	28.0	29.0	34.0 (16.0)	506.0 (33.0)
standard deviation $\xi \cdot 10^2 / \mu\text{m}$	4.9	5.9	7.9	12.6	18.8	25.4	163.2
shape factor Ψ	0.53	0.69	0.73	0.79	0.94	0.93 (0.63)	0.90 (0.51)
intercept length in x $d_x \cdot 10^2 / \mu\text{m}$	8.7	11.1	24.0	31.0	38.0	40.0 (16.0)	520.0 (39.0)
intercept length in y $d_y \cdot 10^2 / \mu\text{m}$	8.2	8.2	22.0	33.0	30.0	43.0 (15.0)	749.0 (24.0)
No. of analyzed particles	782	855	848	419	136	110	90
vol. fraction of MnO_2 phase / %	/	/	/	/	/	1.16	3.94

$= 1 - \rho/\rho_0$) and from the quantitative microstructure analysis ε' . Both values, ε and ε' , are in relatively good agreement. The sintering temperature also substantially influences the size of the LSM particles. The mean particle size in each case was determined as a diameter of the area analogue circle \bar{d} as well as the intercept length in the x or y directions d_x and d_y . With increasing sintering temperatures, all the values \bar{d} , d_x and d_y increased and the LSM particles become increasingly

spherical (shape factor Ψ). As mentioned previously, temperatures above 1100 °C may cause re-precipitation of the secondary phase MnO_2 . The values \bar{d} , d_x , d_y and Ψ describing the formed MnO_2 particles are summarized in **Table 1** in brackets.

Since the LSM in SOFC applications is prepared as a relatively thin porous layer, it is necessary to establish the relationship between the material's microstructure and its electrical characteristics. The appropriate electrical conductivity of the material prepared as a dense element is one of the principal requirements. However, considering only the electrical conductivity data of the dense element without relating this data to the real material microstructure is insufficient. The electrical conductivity of the porous material is described not only by its specific electrical conductivity σ_0 but also by the element's relative density and the degree of connection between the particles along the potential gradient. In this respect, the sine-wave approximation considers a highly porous ceramic element as the repeating pattern of a uniaxial string of spheres. In this simplified approach to describing the microstructure, the volume of the rotating string is controlled by the contribution of two sine-waves. The progress of the sintering is described by changing the ratio of the contribution of the two sine-waves to the string volume (changing the parameter c as described by Mizusaki et al²³). Finally, the change of the relative specific electrical conductivity σ/σ_0 vs. the change in the material's relative density ρ/ρ_0 can be presented.

Results describing the apparent conductivity of the sintered materials vs. the temperature with respect to their relative density or porosity are shown in **Figure 5**. The apparent conductivity increases with temperature, indicating the semi-conductive nature of the LSM ceramics. Since the LSM's density was controlled through a sintering process (higher densities were obtained if T_s was higher) it was to be expected that the specific conductivities σ should also reach higher values with progress in the particle-to-particle contact. As an

**Figure 4:** Microstructure of LSM elements sintered at various temperatures**Slika 4:** Mikrostruktura LSM-tabletk, sintranih pri različnih temperaturah

absolute value, the highest $\sigma = 65 \text{ S/cm}$ at $800 \text{ }^\circ\text{C}$ was measured for a sample with $\rho/\rho_0 = 99.58 \%$.

The relationship relative conductivity (σ/σ_0) vs. relative density (ρ/ρ_0) or porosity (ϵ) is demonstrated in **Figure 6**. For the σ_0 value, the highest measured σ value was adopted ($\sigma_0 = 65 \text{ S/cm}$), while ρ_0 was the theoretical density of $\text{La}_{0.85}\text{Sr}_{0.15}\text{MnO}_3$ ($\rho_0 = 6.595 \text{ g/cm}^3$). The observed results of the relative conductivity σ/σ_0 vs. relative density ρ/ρ_0 dependence are essentially consistent with the sine-wave approximation of the conductivity change for porous materials. The scattering of the observed results around the theoretically predicted curves may be attributed to the inaccuracy of the conductivity measurements or some microstructure defects in the measured bodies. Because of the simplification of the sine-wave modeling regarding the material's microstructure, it is impossible to discuss precisely the relationship between the theoretical predictions and the experimental results. That is to say, contrary to the assumption used in the mathematical model, the grain size and shapes are not homogeneous and the packing of the grains is disordered. To incorporate the inhomogeneity and disorder, such as micro-cracks, the low-scale material inhomogeneity, the inhomogeneous grain size and shape or the local packing disorder into the sine-wave model, a more advanced approach to a mathematical description of the microstructure will be needed.

However, a comparison of the results presented in **Figure 6** revealed that the LSM's relative conductivity convergences on 0 at the relative density 0.45–0.55, a value close to the relative density of as-pressed powders (green density). Such a relationship is not surprising; ceramics are generally prepared from green parts that consist of isolated particles of material. In as-pressed powders, the particles are isolated, except for the

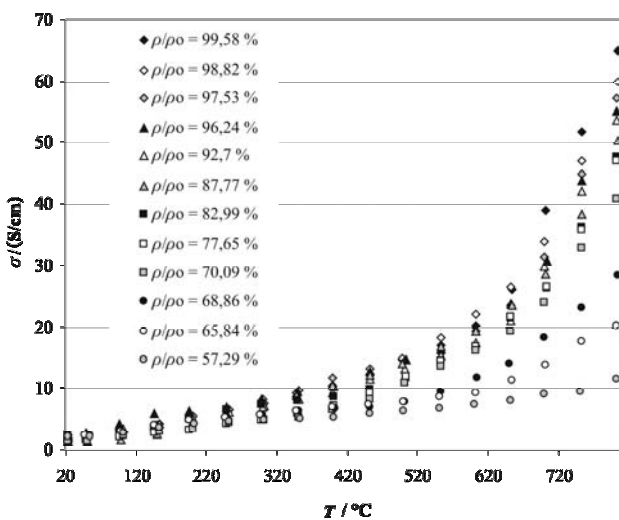


Figure 5: Specific conductivity vs. temperature for a series of LSM elements cermet with various relative densities

Slika 5: Specifična prevodnost LSM-keramike različne relativne gostote kot funkcija temperature

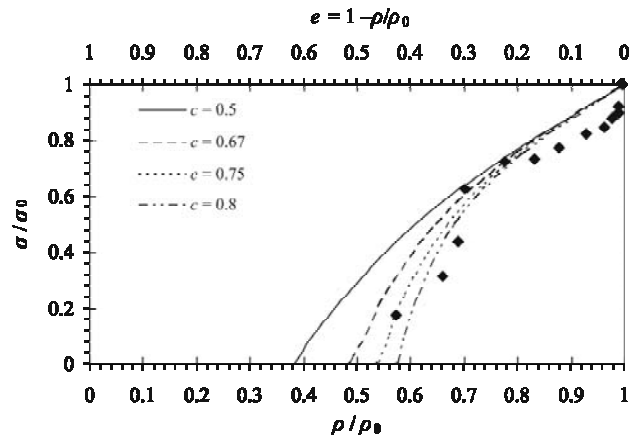


Figure 6: Calculated relationships between the relative conductivity σ/σ_0 and the relative density ρ/ρ_0 or porosity ϵ for different parameters c ; (solid, dashed and dotted lines as described by Mizusaki et al²⁵) and the observed trend of the measured data (\blacklozenge LSM tablets). The relative shape parameter c determines the contribution of the two sine-waves in describing the shape of the cross-section of the particle during sintering.

Slika 6: Odnos med relativno prevodnostjo σ/σ_0 in relativno gostoto ρ/ρ_0 oziroma poroznostjo ϵ LSM-tablet z ozirom na mikrostrukturni parameter c (polna in črtkane črte). Parameter c določa prispevek obeh sinusnih funkcij, ki opisujeta obliko delca med sintranjem.

point-contacts between them, i.e., it is not the material but the void space that is continuous. The electrical conduction in green wares is strongly hindered by the limited contact between the particles, although the apparent density is normally in the range 40–60 %. With increasing sintering temperatures, the relative sintered densities increase, ensuring a better contact between the particles, which is demonstrated through higher relative conductivities.

4 CONCLUSIONS

LSM was prepared using the carbonate co-precipitation route. The relatively small amount of secondary phases in the synthesized and subsequently calcined sample up to $1000 \text{ }^\circ\text{C}$ makes the co-precipitation method favorable when compared to synthesis processes that are based on the diffusion of components in the solid state. During LSM sinterability tests, the best results were achieved when a combination of milling methods was used (grinding in an agate mortar, wet milling in a ball mill and attritor milling). Such combinations of homogenization operations may substantially lower the sintering temperature of the LSM tablets. Rather dense elements, with relative densities greater than 92 %, can be prepared at sintering temperatures T_s as low as $1090 \text{ }^\circ\text{C}$. The electrical conductivity behavior of the prepared LSM bodies was determined with respect to the material's microstructure characteristics. The apparent conductivity of the prepared LSM bodies increased with temperature, indicating their semi-conductive nature. The relationship between the relative conductivity (σ/σ_0) vs. the relative density (ρ/ρ_0) or the porosity (ϵ) was essentially con-

sistent with the sine-wave approximation of conductivity change for porous materials.

5 LITERATURE

- ¹ M. Kakihana, Sol-gel preparation of high temperature superconducting oxides, *J. Sol-Gel Sci. Technol.*, 6 (1996), 7–55
- ² N. Q. Minh, Ceramic Fuel Cells, *J. Am. Ceram. Soc.*, 76 (1993), 563–588
- ³ B. C. H. Steele, Material science and engineering: the enabling technology for the commercialization of fuel cell systems, *J. Mater. Sci.*, 36 (2001), 1053–1068
- ⁴ M. L. Perry, T. F. Fuller, A historical perspective of fuel cell technology in the 20th century, *J. Electrochem. Soc.*, 149 (2002), S59–S67
- ⁵ R. Mahesh, R. Mahendiran, A. K. Raychaudhuri, C. N. R. Rao, Effect of particle size on the giant magnetoresistance of $\text{La}_{0.7}\text{Ca}_{0.3}\text{MnO}_3$, *Appl. Phys. Lett.*, 68 (1996), 2291–2293
- ⁶ Y. Huang, Z. Xu, C. Yan, Z. Wang, T. Zhu, C. Liao, Soft chemical synthesis and transport properties of $\text{La}_{0.7}\text{Sr}_{0.3}\text{MnO}_3$ granular perovskites, *Solid State Commun.*, 114 (2000), 43–47
- ⁷ N. Zhang, W. Ding, W. Zhong, D. Xing, Y. Du, Tunnel-type giant magnetoresistance in the granular perovskite $\text{La}_{0.85}\text{Sr}_{0.15}\text{MnO}_3$, *Phys. Rev.*, B56 (1997), 8138–8142
- ⁸ A. Chakraborty, P. S. Devi, S. Roy, H. S. Maiti, Low-temperature synthesis of ultrafine $\text{La}_{0.84}\text{Sr}_{0.16}\text{MnO}_3$ powder by an autoignition process, *J. Mater. Res.* 9 (1994), 986–991
- ⁹ P. A. Lessing, Mixed-cation oxide powders via polymeric precursors, *Ceram. Bull.* 68 (1989), 1002–1007
- ¹⁰ H.U. Anderson, Review of p-type doped perovskite materials for SOFC and other applications, *Solid State Ionics* 52 (1992), 33–41
- ¹¹ K. Prabhakaran, J. Joseph, N. M. Gokhale, S. C. Sharma, R. Lal, Sucrose Combustion Synthesis of $\text{La}_x\text{Sr}_{1-x}\text{MnO}_3$ ($x \leq 0.2$) powders, *Ceramics International*, 31 (2005), 327–331
- ¹² Y. Huang, Z. Xu, C. Yan, Z. Wang, T. Zhu, C. Liao, Soft chemical synthesis and transport properties of $\text{La}_{0.7}\text{Sr}_{0.3}\text{MnO}_3$ granular perovskites, *Solid State Commun.*, 114 (2000), 43–47
- ¹³ S. Bilger, E. Syskakis, A. Naoumidis, H. Nickel, Sol-Gel Synthesis of Strontium-Doped Lanthanum Manganite, *J. Am. Ceram. Soc.* 75 (1992), 964–970
- ¹⁴ Y. Shimizu, T. Murata, Sol-gel synthesis of perovskite-type lanthanum manganite thin films and fine powders using metal acetylacetonate and poly(vinyl alcohol), *J. Am. Ceram. Soc.* 80 (1997), 2702–2704
- ¹⁵ M. Gaudon, C. Laberty-Robert, F. Ansart, P. Stevens, A. Rousset, Preparation and characterization of $\text{La}_{1-x}\text{Sr}_x\text{MnO}_{3+\delta}$ ($0 \leq x \leq 0.6$) powder by sol-gel processing, *Solid State Sciences*, 4 (2002), 125–133
- ¹⁶ P. Kuttan; J. Jorly; G. N. Madhusudan, S.S. Chandra, L. Ramji, Synthesis of nanocrystalline lanthanum strontium manganite powder by the urea-formaldehyde polymer gel combustion route, <http://www.ingentaconnect.com/content/bsc/jace;jsessionid=54t7kd2r5airk.alexandra> "Journal of the American Ceramic Society", 89 (2006) 7, 2335–2337
- ¹⁷ M.B. Kakade, S. Ramanathan, G.K. Dey, D. Das, Processing and Characterisation of Porous Lanthanum Strontium Manganite -Role of Porosity on Electrical Conductivity and Morphology, *Advances in applied ceramics*, 107 (2008) 2, 89–95
- ¹⁸ A. M. Duprat, P. Alphonse, C. Sarda, A. Rousset, B. Gillot, Non-stoichiometry-activity relationship in perovskite-like manganites, *Mater. Chem. Phys.* 37 (1994), 76–81
- ¹⁹ A. Ghosh, A. K. Sahu, A. K. Gulnar, A. K. Suri, Synthesis and Characterization of Lanthanum Strontium Manganite, *Scripta Materialia*, 52 (2005), 1305–1309
- ²⁰ J. Sfeir, S. Vaucher, P. Holtappels, U. Vogt, H.-J. Schindler, J. Van herle, E. Suvorova, P. Buffat, D. Perret, N. Xanthopoulos, O. Bucheli, Characterization of perovskite powders for cathode and oxygen membranes made by different synthesis routes, *Journal of the European Ceramic Society*, 25 (2005), 1991–1995
- ²¹ R. J. Bell, G. J. Millar, J. Drennan, Influence of synthesis route on the catalytic properties of $\text{La}_{1-x}\text{Sr}_x\text{MnO}_3$, *Solid State Ionics*, 131 (2000), 211–220
- ²² J. Tanaka, K. Takahashi, Y. Yajima, M. Tsukioka, Lattice constants of monoclinic $(\text{La}_{0.8}\text{Ca}_{0.2})\text{MnO}_3$, *Chemistry Letters*, (1982), 1847–1850
- ²³ A. Chakraborty, P. Choudhury, H. S. Maiti, Electrical conductivity in Sr-substituted lanthanum manganite cathode material prepared by autoignition technique, Proc. 4th Int. Symp. On SOFC, (Ed. M. Dokiya, O. Yamamoto, H. Tagawa, S.C. Singhal), (1995), 612–618
- ²⁴ N. Q. Minh, T. Takahashi, Science and technology of ceramic fuel cells, Elsevier, The Netherlands, 1995
- ²⁵ J. Mizusaki, S. Tsuchiya, K. Waragi, H. Tagawa, Y. Arai, Y. Kuwayama, Simple mathematical model for the electrical conductivity of highly porous ceramics, *J. Am. Ceram. Soc.*, 79 (1996) 1, 109–113
- ²⁶ L. Kilizendermann, D. Das, D. Bahadur, R. Weiss, H. Nickel, K. Hilpert, Chemical interaction between La-Sr-Mn-Fe-O based perovskites and Yttria stabilized Zirconia, *J. Am. Ceram. Soc.*, 80 (1997) 4, 909–914
- ²⁷ C. Clausen, C. Bagger, J. B. Bilde-Sorensen, A. Horsewell, Microstructural and microchemical characterization of the interface between $\text{La}_{0.85}\text{Sr}_{0.15}\text{MnO}_3$ and Y_2O_3 -stabilized ZrO_2 , *Solid State Ionics*, 70/71 (1994), 59–64